Mausam, (1986), 37, 1, 103-106

551.553.21:551.46.062.6

Response of the upper layers of the Arabian Sea and the Bay of Bengal to the southwest monsoon

T. K. RAY

Meteorological Office, New Delhi

(*Received 25 August 1984*)

सार — इस लेख में मानसून के विभिन्न चरणों में महासागरों की ऊपरी परतों की प्रतिक्रिया का अध्ययन किया गया है । मानसून-पूर्व, कमजोर मानसून या मानसून के बीच में व्यवधान वाली अवधियों में पुरवाई पवनों की शक्ति कम होती है और वह पछुआ बनने लगती है। मानसून के आरंभ के चरण में पछुआ अवश्य गहराई के साथ सशक्त होने लगता है। आरंभ से पूर्व की अथवा कमजोर मानसून की अवधि में निर्बल धनात्मक या ऋणात्मक भ्रामिलता प्रमुख होती है जबकि मानसून की सक्रियता के समय सशक्त धनात्मक भ्रमिलता अरब सागर पर छा जाती है। मानसून के विभिन्न चरणों में गतिज ऊर्जा, अपसरण तथा ऊर्ध्वाधर सदिश गति प्रतिदर्श भी दिलचस्प घटनाचक्र दिखाते हैं।

ABSTRACT. Response, to the monsoon in its various phases, of the upper layers of the oceans has been studied in this paper. During pre-monsoon and weak or break monsoon periods the strength of the easterly current reduces and tends to become westerly. During onset phase westerly component increases with depth. While weak positive or negative vorticity predominates during pre-onset or break periods, strong positive vorticity rules the Arabian Sea during active monsoon. Kinetic energy, divergence and vertical velocity patterns also show interesting behaviour during various phases of monsoon.

1. Introduction

Many changes occur in the surface features of the Arabian Sea and the Bay of Bengal during pre and post onset phases of monsoon. Changes on the surface in the form of sea and swell have been studied by many (Venkiteswaran 1960, Mukherjee and Sivaramakrishnan 1976). Raghavan (1969) suggested that a relation may possibly exist between weak or even break monsoon condition with the upwelling of east Arabian Sea waters off west coast of India. His explanation was based on the fact that during weak monsoon surface winds over eastern Arabian Sea are generally northerly or northnorthwesterly, *i.e.*, parallel to the coast; such winds are favourable for coastal upwelling. La Fond and Borreswara Rao (1955) observed coastal sinking during October in the eastern coast of India. But all these studies were based on limited data. The dynamics and kinematics of the sub-surface layers display spectacular variations. These changes that occur in the depths of the oceans with the approach of monsoon and later in the season have not been extensively studied due mainly to lack of adequate data.

2. Data and analysis

During the monsoon experiment (MONEX-79) in the summer of 1979 five USSR ships recorded observations in the depths of the Arabian Sea and the Bay of Bengal in three stationary polygon positions. Flow of water (cm/sec) at depths of 25, 50, 100, 150, 200, 300, 400, 500 and 800 m twice (00 & 12 GMT) daily have been analysed. Mean flow between two levels has been linearly interpolated whenever needed.

In order to keep consistency with air flow, flow of water also has been considered from the direction it is arriving instead of the usual way — the direction to which it is flowing. Westerly and southerly components have been taken positive while northerly and easterly are negative.

Analysis of the data and interpretation of results made in three phases are as follows :

Phase I—16 to 29 May (pre-onset).
Phase II—2 to 14 June (onset).
Phase III—10 to 23 July (break-monsoon).

Mean kinetic energy at the locations have been computed in the usual way :

$$\text{K. E.} = \frac{1}{2}\left(\bar{u}^2 + \bar{v}^2\right)^{\frac{1}{2}},$$ where $\bar{u}$ and $\bar{v}$ are the mean zonal and meridional components of flow between two levels within the polygons.

At each level horizontal divergence and vertical component of relative vorticity were calculated as flux and circulation per unit area respectively over the polygonal

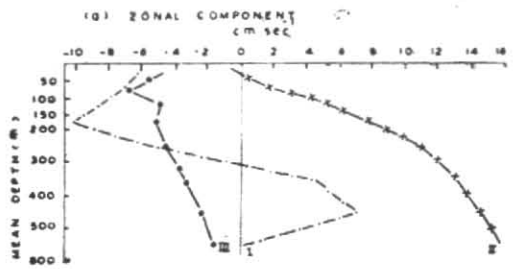

Figs. 1 (a & b.)- Average (a) zonal component and (b) meridional component of water flow (cm sec^{-1})

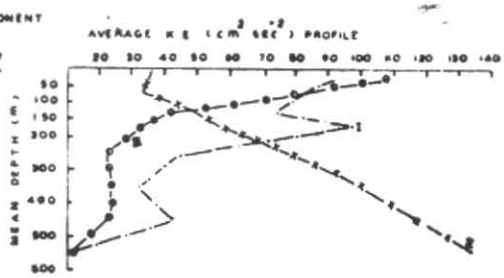

Fig. 2. Average kinetic energy profile

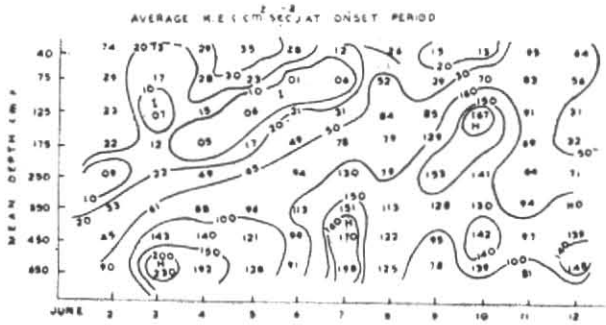

Fig. 3. Daily average kinetic energy (cm^2 sec^{-2}) at onset periods

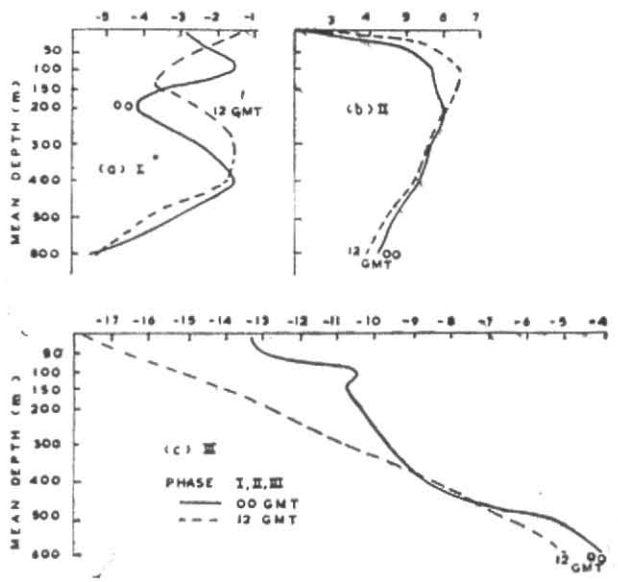

Fig. 4. Vorticity (10^{-5}) at depths during three phases : (a)—I, (b)—II and (c)—III

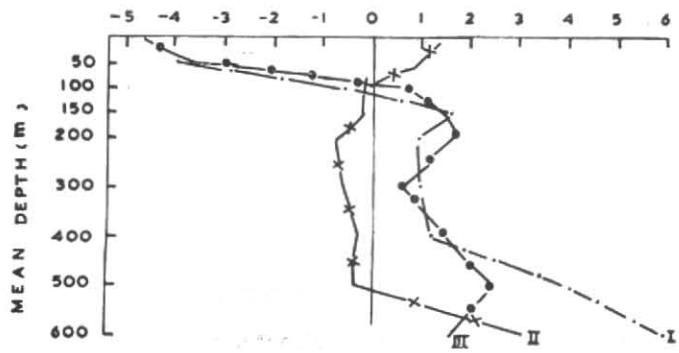

Fig. 5. Average divergence (10^{-5})

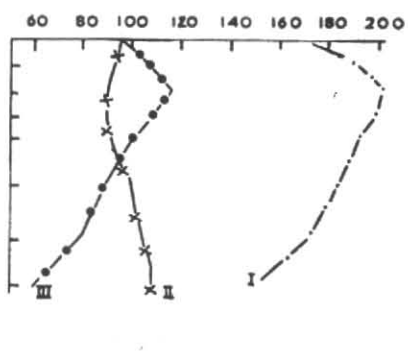

Fig. 6. Average vertical velocity ($10^{-4} ms^{-1}$)

region. The total flux and circulation were computed by contour integration over the polygon as follows :

$$\text{Flux} = \oint v_n \, dl = \sum_{k=1}^{4} \bar{v}_{nk} \, l_k \qquad (1)$$

$$\text{Circulation} = \oint v_r \, dl = \sum_{k=1}^{4} \bar{v}_{rk} \, l_k \qquad (2)$$

where $\bar{v}_{nk}$ and $\bar{v}_{rk}$ are the mean flow components in the normal and radial directions respectively over the kth side of the polygon and l_k is the length of the kth side. To obtain the proper sign for relative vorticity, integration was performed in the anti-clockwise direction. In a few cases, when the data from only three ships were available, the integration over the triangle was performed. Data from less than three ships have not been considered for analysis.

Vertical velocity W was obtained by vertical integration of the equation :

$$W = \int_{800}^{25} \nabla . \mathbf{V} \, dh + W_0 \qquad (3)$$

The lower boundary condition was taken as $W_0 = 0$ at 800 m and integration performed for different layers every day at 00 and 12 GMT hours. However, to save space, only average values have been presented.

3. Interpretation of results

3.1. *Components of waterflow*

Figs. 1 (a & b) show the zonal and meridional components of the flow. It is seen that during phase I the strength of the easterly current reduces with depth and tends to become westerly indicating intense vertical circulation through the upper layers of western Arabian Sea in May. In phase I we noted the depth of strongest easterly at 200 m while that for the westerly it is between 400 and 500 m. In phase III (Bay of Bengal) we observe strongest easterly at 100 m, thereafter its strength is gradually reduced upto 800 metres. A quite contrasting picture is noticed in phase II (onset of monsoon over Kerala coast). Here we note predominantly westerly components whose intensity increases with depth reaching almost 16 cm/sec at 800 m. From the meridional component diagram we can see weak southerly more predominant in phase I and phase III. In phase II we note weak northerlies below 50 m depth.

3.2. *Kinetic Energy (K.E.)*

Kinetic energy profiles through the depths of the Arabian Sea and the Bay of Bengal have been presented in Fig 2. From the diagram we note the following :

(a) During phase I and phase III the K.E. decreases with depth reaching a minimum value at the lowest layer considered. Maximum K.E. is seen in the near-surface layer between 25 and 50 metres in phase III.

(b) During phase I, two maxima are visible : one between 150 and 200 m depth. Minimum K.E for phase I almost coincides with that for phase III.

(c) Phase II presents a completely different picture for average K.E. Starting from a small value of 35 cm^2/sec^2 in the upper layers the K.E. sharply increases with depth until it reaches a maximum value of 135 cm^2/sec^2 at the lowest layer considered.

The change in K.E. from phase I to phase II, where time difference is only 4 days (last day of phase I is 29 May and the first day of phase II is 2 June) and space difference between two polygons is about 1100 km, is noteworthy. This is very interesting in view of the fact that the southwest monsoon rains burst over Kerala coast on 11 June 1979. The centre of the ships polygon II was about 1000 km away from the west coast of India.

From the daily average K.E. chart (Fig. 3) we note that the highest K.E. in the uppermost layers are registered on 9 and 10 June. It also emerges from this diagram that the level of maximum K.E. rises on the eve of monsoon onset. From 3 June when conditions start getting favourable for the onset, the K.E. at deeper layers start increasing and on 9-10 June the maximum K.E. is noticed around 125 m below sea surface. This only shows that along with the onset of monsoon over India, ocean current off Indian coast also strengthens and grows in vertical extent.

3.3. *Relative vorticity*

Though basic vorticity patterns remained similar, minor diurnal variations are noticed and so in Fig. 4 both 00 and 12 GMT profiles have been presented. From Fig. 4 we note :

(a) Vorticity is negative throughout the depths in phase I and III.

(b) A complete reversal of vorticity patterns is noticed during phase II—it being strongly positive and the 12 GMT values were marginally higher than the corresponding values at 00 GMT in the upper layers.

(c) In phase III very strong negative vorticity near surface layers weakens with depth. Strong departure between 00 and 12 GMT can also be noticed.

From the above one can conclude that during the build-up or weak/break phases of monsoon, negative vorticity dominates whereas strong positive vorticity prevails during the onset or active phase of monsoon.

3.4. *Divergence*

Average divergence profiles for 00 and 12 GMT have been presented in Fig. 5. Here also one notices similarity of patterns between phase I and phase III. Infact, upto a depth of 400 m both curves almost coincide. Below this level divergence increases very steeply in phase I while in phase III it reaches a maximum at 500 m and then decreases gradually. Over the upper

layers strong convergence is noticed in these two phases and at around 100 m convergence changes to divergence. Looking at the phase II graph one identifies dynamically more active layers. Here we see upper (near-surface) and deeper layers have divergent flows while the middle layers between 100 m and 500 m have converging flows. Drawing analogy from atmosphere, we see that the 'level of non-divergence' lies at around 100 m in all the three phases.

3.5. *Vertical velocity*

Mean vertical velocity profile can be seen in Fig. 6. In phase I we see strong vertical motion (upwelling) taking place. Strongest vertical velocity ($2/10^2$ cm/sec) in polygon I is seen at 100 m depth. This gradually reduces in the lower layers to a minimum ($1.5/10^2$ cm/sec) at 500 m depth.

In polygon II which is closer to Indian coast we note an almost uniform upwelling rate ($1/10^2$ cm/sec) throughout the depth considered.

In the Bay of Bengal polygon during break monsoon period upwelling is maximum ($1.2/10^2$ cm/sec) at 100 m depth. This reduces sharply, and we not an upwelling rate of $0.6/10^2$ cm/sec in the lowest layer considered.

Thus, the upwelling is maximum in polygon I because of its proximity to eastern coast of Africa. The upwelling is reasonably high even in polygon II, which is far away from east Africa coast, due to strong monsoon current during the onset phase. One other important fact is that the upwelling is maximum near 100 m in all the three phases of monsoon.

4. Conclusion

Though it is difficult to draw any firm conclusion based on one year's data, we noticed some response of the monsoon to the upper layers of the seas. We found :

(*i*) Responses for pre-monsoon and weak monsoon are similar.

(*ii*) Convergence in shallow layers and divergence in deeper layers.

(*iii*) Negative vorticity during pre-onset and weak monsoon periods with strong positive vorticity during active monsoon periods.

(*iv*) Kinetic energy increases with depth in active monsoon period while it decreases with depth during pre-onset or weak monsoon periods.

References

La Fond, E.C. and Rao, Borreswara C., 1955, 'Vertical temperature structure of the upper layers of the sea off east coast of India', Defence Sci. Organisation No. 4/55.

Mukherjee, A.K. and Sivaramakrishnan, T.R., 1976, 'A narrow band of high swells over the Arabian Sea as a precursor of monsoon', Proc. symp. on tropical monsoon, Pune, 166-169.

Raghavan, K., 1969, 'Satellite evidence of air-sea interactions during Indian monsoon', *Mon. Weath. Rev.*, **97**, 12, 905-908

Venkiteswaran, S.P., 1960, 'Swells in the Bay of Bengal associated with storms in November', *Indian J. Met. Geophys.*, **11**, 30-34.